Electronic Supplementary Material (ESI) for Dalton Transactions.


Supplementary Information

# Correlating Cobalt Redox Couples to Photovoltage in the Dye-Sensitized Solar Cell

Kitty Y. Chen, [a] Phil A. Schauer,[a] Brian O. Patrick, [a] and Curtis P. Berlinguette*[a,b]

[a]Department of Chemistry, University of British Columbia, 2036 Main Mall, Vancouver, British Columbia, V6T 1Z1, Canada.

[b]Department of Chemical & Biological Engineering, University of British Columbia, 2360 East Mall, Vancouver, British Columbia V6T, Canada.

[c]Stewart Blusson Quantum Matter Institute, The University of British Columbia, 2355 East Mall, Vancouver, BC V6T 1Z4, Canada.

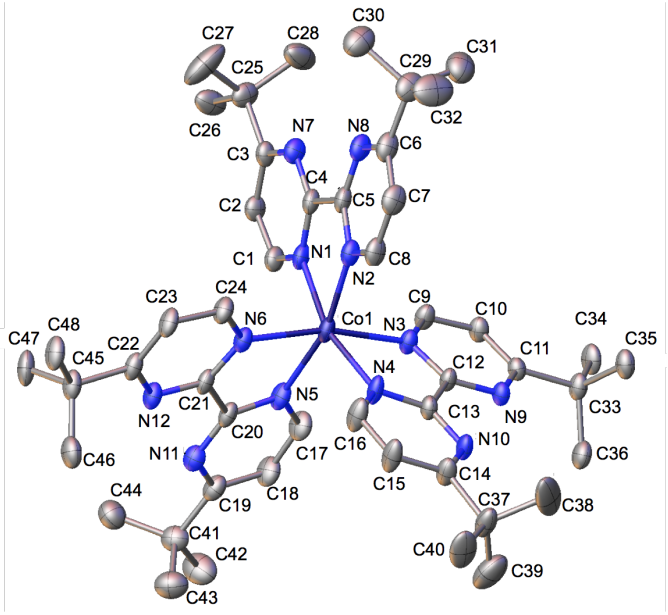


**Figure S1.** Thermal ellipsoid plot of [**Co-(bpm-DTB)**]$^{2+}$ drawn at the 50% probability level.

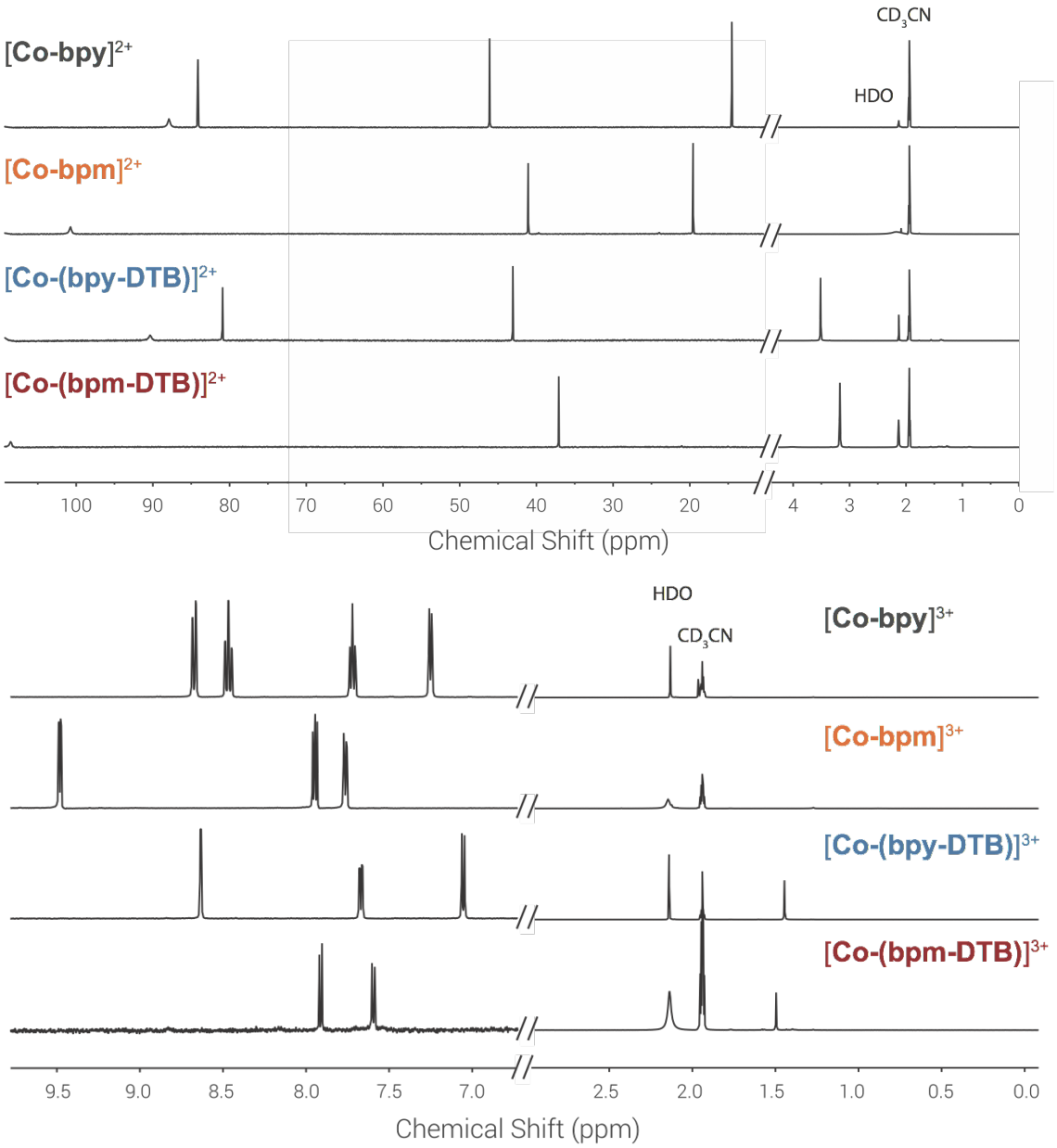


**Figure S2.** $^{1}$H NMR spectra of paramagnetic species **[Co-bpy]**$^{2+}$, **[Co-bpm]**$^{2+}$, **[Co-(bpy-DTB)]**$^{2+}$, and **[Co-(bpm-DTB)]**$^{2+}$ and diamagnetic species **[Co-bpy]**$^{3+}$, **[Co-bpm]**$^{3+}$, **[Co-(bpy-DTB)]**$^{3+}$, and **[Co-(bpm-DTB)]**$^{3+}$ in $CD_3CN$. Note that the peak heights are not scaled equally at low and high chemical shift ranges.

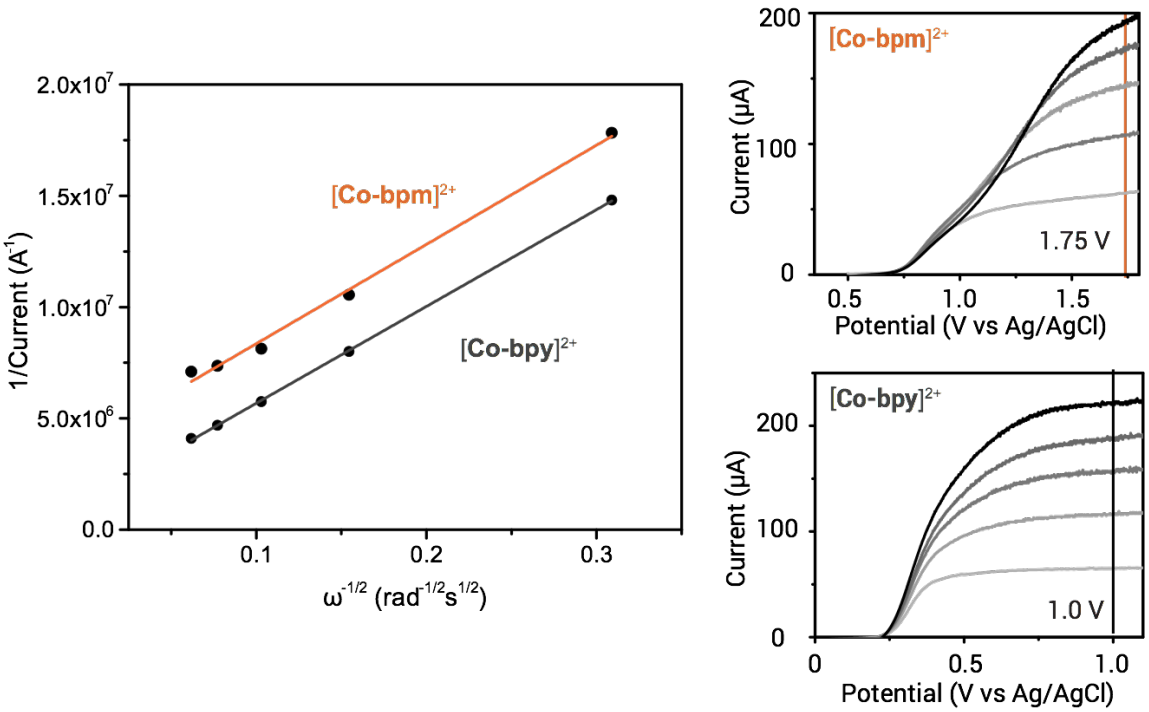


**Figure S3.** Levich-Koutecky plots of [**Co-bpm**]$^{2+}$ and [**Co-bpy**]$^{2+}$. The corresponding the linear sweep voltammetry (LSV) traces are shown on the right with vertical line indicating the potential at which the currents are taken. Traces were swept at 100 mV/s in a three-electrode set up: Ag/AgCl reference electrode, rotating GC working electrode, and Pt counter electrode in 0.1 M $NBu_4PF_6$ dissolved in MeCN.

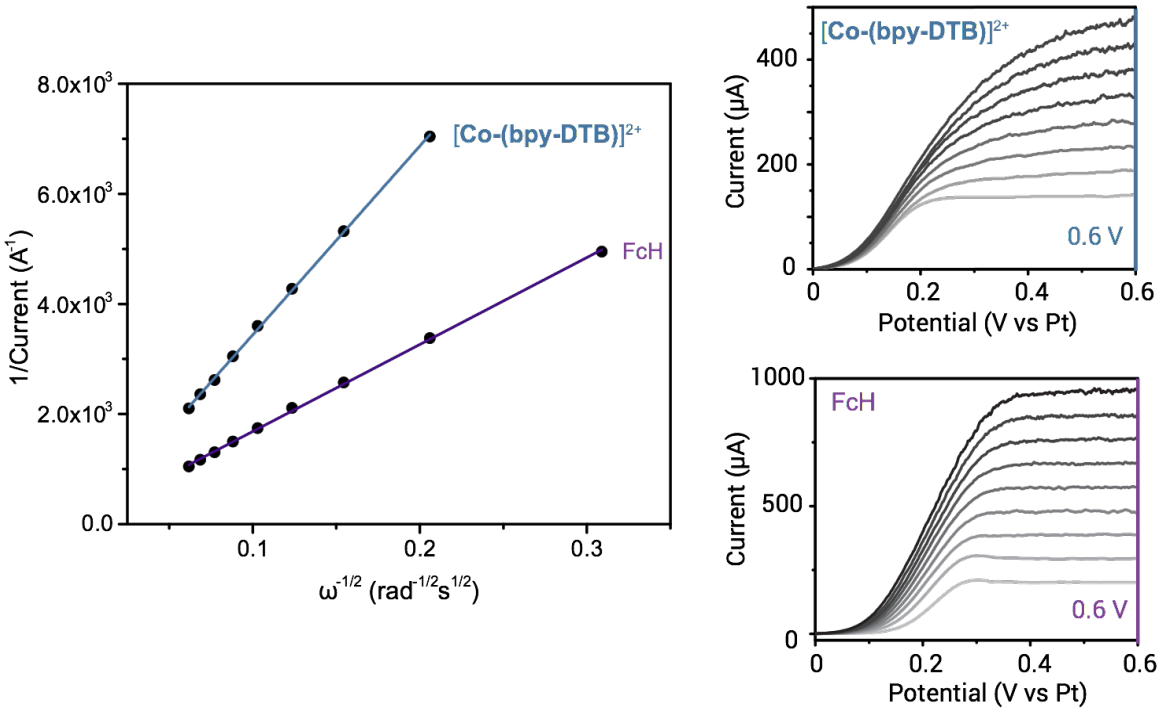


**Figure S4.** Levich-Koutecky plots of [**Co-(bpy-DTB)**]$^{2+}$ and ferrocene (FcH). The corresponding the linear sweep voltammetry (LSV) traces are shown on the right with vertical line indicating the potential at which the currents are taken. Traces were swept at 100 mV/s in a three-electrode set up: Ag/AgCl reference electrode, rotating Au working electrode, and Pt counter electrode in 0.1 M $NBu_4PF_6$ dissolved in MeCN.

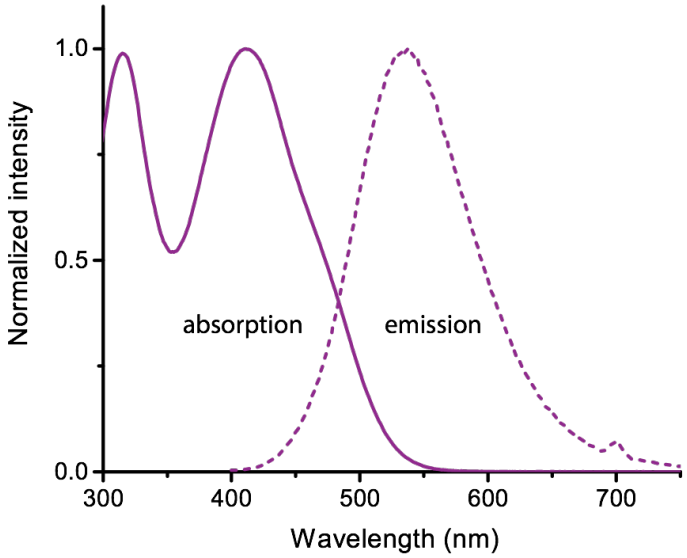


**Figure S5.** Normalized UV-vis absorption and emission spectra of **Dye-I**. $E_{0\text{-}0}$ is estimated from the intersection of absorbance and emission spectra. Excitation wavelength: 350 nm; slit width: 5 nm.

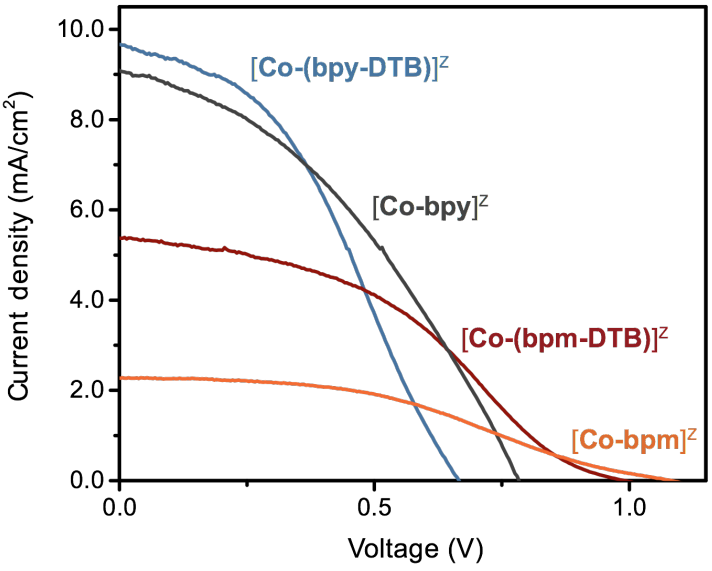


**Figure S6.** Best performing J-V curves of devices containing [**Co-(bpy-DTB)**]$^Z$ (blue), [**Co-bpy**]$^Z$ (grey), [**Co-(bpm-DTB)**]$^Z$ (red), and [**Co-bpm**]$^Z$ (orange). The performance of two replicate devices for each type of mediator were plotted.

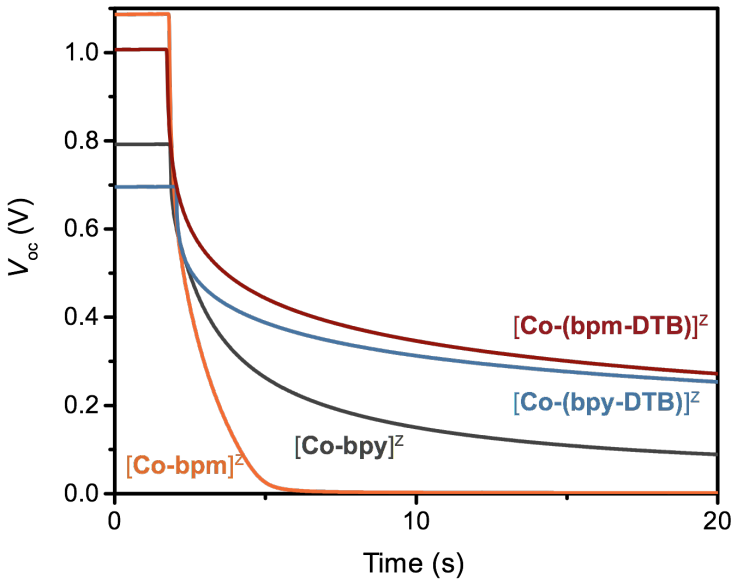


**Figure S7.** OCVD decay curve measured in devices containing **Co-bpm** (orange), **Co-bpy** (grey), **Co-(bpm-DTB)** (red) and **Co-(bpy-DTB)** (blue).

**Table S1.** Crystallographic Data for **[Co-(bpm-DTB)]**$(PF_6)_2$

| | | | |
|---|---|---|---|
| Chemical formula | $C_{54}H_{75}CoN_{15}F_{12}P_2$ | Formula weight | 1279.05 |
| a | 10.9787(11) Å | Space group | $P2_1/n$ (#14) |
| b | 21.384(3) Å | T | -173 °C |
| c | 28.322(3) Å | λ | 0.71073 Å |
| α, β, γ | 90°, 99.957(5)°, 90° | $D_{calcd}$ | 1.297 g/cm$^3$ |
| V | 6551.1(13) Å$^3$ | μ | 3.91 cm$^{-1}$ |
| Z | 4 | $R_1$[a]; $wR_2(I>2.00\sigma(I))$[b] | 0.0593; 0.1158 |
| | | $R_1$[a]; $wR_2$(all data)[b] | 0.0770; 0.1215 |

[a]$R_1 = \sum ||F_o| - |F_c|| / \sum |F_o|$, [b]$wR_2 = [\sum ( w (F_o^2 - Fc^2)^2)/ \sum(w(F_o^2)^2)^{1/2}$

**Table S2.** Selected Bond Lengths [Å] and Angles [°] for [**Co-(bpm-DTB)**]$(PF_6)_2$

| Atom | Atom | Bond length |
|---|---|---|
| | | Å |
| Co1 | N1 | 2.126(3) |
| Co1 | N2 | 2.149(3) |
| Co1 | N3 | 2.158(3) |
| Co1 | N4 | 2.127(3) |
| Co1 | N5 | 2.147(3) |
| Co1 | N6 | 2.158(3) |

| Atom | Atom | Atom | Bond angle |
|---|---|---|---|
| | | | ° |
| N1 | Co1 | N2 | 76.48(10) |
| N1 | Co1 | N3 | 92.10(10) |
| N1 | Co1 | N4 | 163.78(11) |
| N1 | Co1 | N5 | 95.86(11) |
| N1 | Co1 | N6 | 97.29(10) |
| N2 | Co1 | N3 | 99.64(10) |
| N2 | Co1 | N6 | 92.00(10) |
| N3 | Co1 | N6 | 166.50(11) |
| N4 | Co1 | N2 | 93.87(11) |
| N4 | Co1 | N3 | 76.49(10) |
| N4 | Co1 | N5 | 96.22(11) |
| N4 | Co1 | N6 | 96.04(10) |
| N5 | Co1 | N2 | 165.38(7) |
| N5 | Co1 | N3 | 93.0017) |
| N5 | Co1 | N6 | 76.46(7) |

**Table S3**. UV-vis Absorption of [**Co-bpy**]$(PF_6)_2$, [**Co-bpm**]$(PF_6)_2$, [**Co-(bpy-DTB)**]$(PF_6)_2$, and [**Co-(bpm-DTB)**]$(PF_6)_2$ in MeCN

| Compound | $\lambda_{max1}$/nm ($\varepsilon$/$M^{-1}cm^{-1}$) | $\lambda_{max2}$/nm ($\varepsilon$/$M^{-1}cm^{-1}$) | $\lambda_{max3}$/nm ($\varepsilon$/$M^{-1}cm^{-1}$) | $\lambda_{max4}$/nm ($\varepsilon$/$M^{-1}cm^{-1}$) | $\lambda_{max5}$/nm ($\varepsilon$/$M^{-1}cm^{-1}$) |
|---|---|---|---|---|---|
| [**Co-(bpy-DTB)**]$(PF_6)_2$ | 248 ($3.51\times 10^4$) | 294 ($3.91 \times 10^4$) | 302 ($3.71\times 10^4$) | 440 ($1.5 \times 10^2$) | 906 (8.8) |
| [**Co-bpy**]$(PF_6)_2$ | 245 ($2.49 \times 10^4$) | 295 ($2.96 \times 10^4$) | 305 ($2.81\times 10^4$) | 440 ($1.1 \times 10^2$) | 901 (6.7) |
| [**Co-(bpm-DTB)**]$(PF_6)_2$ | 248 ($4.78 \times 10^4$) | - | - | 450 (51) | 935 (8.0) |
| [**Co-bpm**]$(PF_6)_2$ | 243 ($4.72\times 10^4$) | - | - | 465 (55) | 935 (7.5) |

**Calculation of magnetic susceptibility and effective magnetic moment**

The total magnetic susceptibility ($X_m$) for each Co(II) complex was calculated using the simplified Evans equation[1] shown in Equation S1 where $\Delta f$ is the frequency shift of the 1,4-dioxane signal seen in the $^1$H NMR spectra in the presence of paramagnetic Co(II) species, $f$ is the NMR spectrometer frequency ($400.00 \times 10^6$ Hz), and $c$ is the concentration of the paramagnetic complex (10 mM). The paramagnetic contribution ($X_p$) of the magnetic susceptibility was obtained by subtracting the diamagnetic contribution ($X_d$) of the magnetic susceptibility (estimated from Pascal's constant[2]) from $X_m$ (Equation S2). The effective magnetic moments ($\mu_{eff}$) were obtained using Equation S3.[149] $k_b$ is Boltzmann constant, $N$ is Avogadro constant, $u_B$ is the Bohr magneton, and $T$ is the temperature (298 K). The relevant magnetic susceptibility parameters for [**Co-bpy**]$^{2+}$, [**Co-bpm**]$^{2+}$, [**Co-(bpy-DTB)**]$^{2+}$, and [**Co-(bpm-DTB)**]$^{2+}$ are tabulated in Table S4,

$$X_m = \frac{3000\Delta f}{4\pi f c} \quad \text{(S1)}$$

$$X_p = X_m - X_d \quad \text{(S2)}$$

$$\mu_{eff} = \sqrt{\frac{3k_b T X_p}{N{u_B}^2}} \approx \sqrt{8 \cdot T X_p} \quad \text{(S3)}$$

**Table S4.** Relevant Magnetic Susceptibility Parameters for [**Co-bpy**]$^{2+}$, [**Co-bpm**]$^{2+}$, [**Co-(bpy-DTB)**]$^{2+}$, and [**Co-(bpy-DTB)**]$^{2+}$.

| Complex | [**Co-bpy**]$^{2+}$ | [**Co-bpm**]$^{2+}$ | [**Co-(bpy-DTB)**]$^{2+}$ | [**Co-(bpy-DTB)**]$^{2+}$ |
|---|---|---|---|---|
| $c$ (mM) | 10.9 | 10.5 | 9.64 | 9.17 |
| $\Delta f$ (Hz) | 177.50 | 178.41 | 141.89 | 154.61 |
| $X_m$ (× $10^{-3}$ emu $mol^{-1}$) | 9.70 | 10.13 | 8.79 | 9.51 |
| $X_d$ (× $10^{-4}$ emu $mol^{-1}$) | 2.96 | 2.32 | 5.80 | 5.35 |
| $X_p$ (× $10^{-3}$ emu $mol^{-1}$) | 9.40 | 9.89 | 8.21 | 8.97 |

## References


1. D. H. Grant, *J. Chem. Educ.*, 1995, **72**, 39.
2. G. A. Bain and J. F. Berry, *J. Chem. Educ.*, 2008, **85**, 532.